Grid-Connected Voltage Source Converter
— Control Principles and Wind Energy Applications

Jan Svensson

Technical Report No. 331

1998

Grid-Connected Voltage Source Converter
— Control Principles and Wind Energy Applications

by

Jan Svensson

Technical Report No. 331

Submitted to the School of Electrical and Computer Engineering
Chalmers University of Technology
in partial fulfilment of the requirements
for the degree of
Doctor of Philosophy

Department of Electric Power Engineering
Chalmers University of Technology
Göteborg, Sweden
Mars 1998

CHALMERS UNIVERSITY OF TECHNOLOGY
Department of Electric Power Engineering
S-412 96 Göteborg
ISBN: 91-7197-610-8
ISSN: 0346 - 718X
Chalmers Bibliotek, Reproservice
Göteborg, 1998

Abstract

The thesis focuses on a forced-commutated voltage source converter (VSC) connected to a grid in a wind energy application. The work consists of four parts. The first part addresses the type of electrical system which should be used in a wind turbine. The conclusion is to use variable-speed wind turbines, due to higher efficiency, lower noise and lower fatigue. If high power quality is demanded, a grid-connected VSC should be used instead of a grid-commutated thyristor inverter. By utilizing the high current control bandwidth of the VSC in a hybrid wind farm, consisting of wind turbines having different electrical systems, a cost-efficient solution is obtained. The VSC is used for reactive power compensation and active filtering, in addition to converting wind power. These additional features cause only a moderate increase in the VSC rating compared with only converting wind power.

In part two, an electrical system in a variable-speed wind turbine, in which the VSC uses the voltage angle control to track the reference voltage of the dc-link, is investigated. The proposed control method is based on a steady-state model of the system, which results in a low bandwidth but which is high enough to operate a wind turbine. To increase the bandwidth, the linear quadratic (LQ) control method has been introduced. Due to sensitivity to current harmonics, an extended Kalman filter has been added to the LQ-controller. Simulations show that the controller operates as expected.

A grid-connected VSC using a discrete vector current controller is investigated in the third part of the thesis. The influences of an incorrect controller tuning and grid voltage harmonics on current frequency responses at an operating point are investigated. The attenuation of low-frequency voltage harmonics decreases when their frequency increases. Furthermore, it is shown that the current controller handles parameter errors satisfactorily. It has been shown that frequency dependent losses in the grid filter affect current frequency responses at high frequencies. A compensation function has been introduced to compensate for non-ideal valves and non-ideal pulse width modulation. The function improves the small-signal current frequency response around an operating point. Also four different synchronization methods, which are adapted to digital controllers, have been investigated. A novel transformation angle detector based on a space vector filter has been introduced. The detector manages phase steps in the grid voltage, and the extended version of the detector also manages frequency changes in the grid better than the extended Kalman filtered detector, in spite of the smaller number of calculations.

The last part of the thesis deals with the current harmonics of a grid-connected VSC. By introducing a third-order LCL-filter as an alternative to an L-filter, current harmonics are decreased. Furthermore, reflections caused by high voltage derivatives are adressed.

Preface

The work presented in this thesis was carried out at the Department of Electric Power Engineering at Chalmers University of Technology. The financial support given by the Swedish National Board for Industrial and Technical Development (NUTEK), through the Wind Power Consortium, is gratefully acknowledged.

I would like to thank my supervisor, Dr. Ola Carlson, for believing in my ideas. Furthermore, many thanks to my industrial adviser Tommy Lejonberg for his support and encouraging guidance in the second half of the project. It is a great honor for me to thank my examiner Professor Jorma Luomi, who has guided me into the academic world.

In the second half of the project, I have worked together with Michael Lindgren who has been coauthor of some of the articles in the thesis. Two people working together in a group can work wonders.

Best regards to my daily sound-board, Dr. Torbjörn Thiringer, and to Kjell Siimon for keeping my computer up-to-date. Finally, I would like to thank the staff at the department.

List of Appended Papers

This thesis is based on the work contained in the following papers:

SECTION 1
Voltage Source Converters in Variable Speed Wind Turbines and Hybrid Wind Parks

1A O. Carlson, A. Grauers, J. Svensson, Å. Larsson, "A Comparison of Electrical Systems for Variable Speed Operation of Wind Turbines," *European Wind Energy Association Conference and Exhibition (EWEC'94)*, Thessaloniki, Greece, 10-14 October 1994, pp. 500-505.

1B J. Svensson, "Possibilities by using a Self-Commutated Voltage Source Inverter Connected to a Weak Grid in Wind Parks," *1996 European Union Wind Energy Conference and Exhibition*, Göteborg, Sweden, 20-24 May 1996, pp. 492-495.

1C J. Svensson, "The Rating of the Voltage Source Inverter in a Hybrid Wind Park with High Power Quality," *European Wind Energy Conference (EWEC'97)*, Dublin, Ireland, 6-9 October 1997, (in press).

SECTION 2
Voltage Angle Control of a Voltage Source Converter

2A J. Svensson, "Voltage Angle Control of a Voltage Source Inverter — Application to a Grid-Connected Wind Turbine," *6th European Conference on Power Electronics and Applications (EPE'95)*, Sevilla, Spain, 19-21 September 1995, Proceedings, Vol. 3, pp. 539-544.

2B J. Svensson, "Simulation of Power Angle Controlled Voltage Source Converter using a Linear Quadratic Method in a Wind Energy Application," *5th Workshop on Computers in Power Electronics, IEEE,* 11-14 August 1996, pp. 157-162.

SECTION 3
Vector Controlled Voltage Source Converter

3A J. Svensson, "Inclusion of Dead-Time and Parameter Variations in VSC Modelling for Predicting Responses of Grid Voltage Harmonics," *7th European Conference on Power Electronics and Applications (EPE'97)*, Trondheim, Norway, 8-10 September 1997, Proceedings, Vol. 3, pp. 216-221.

3B J. Svensson, "Synchronisation Methods for Grid Connected Voltage Source Converter," Submitted to IEE Proceedings Electric Power Applications.

3C J. Svensson, M. Lindgren, "Influence of Non-linearities on the Frequency Response of a Grid-Connected Vector-Controlled VSC," submitted to IEEE Transactions on Industrial Electronics.

SECTION 4
Connecting Fast Switching Voltage Source Converters to the Grid

4 M. Lindgren, J. Svensson, "Connecting Fast Switching Voltage-Source Converters to the Grid — Harmonic Distortion and its Reduction," *IEEE/Stockholm Power Tech Conference*, Stockholm, Sweden, June 18-22 1995, Proceedings, Vol. "Power Electronics," pp. 191-196.

Table of Contents

PART I

THE THESIS

1 Introduction

The utilization of wind energy is an area which is growing rapidly. In Europe, the installed wind power has increased by 36 % each year for 5 years, now. In northern Germany, wind turbine manufacture is the fastest growing industry. Furthermore, wind energy covers 7 % of Danish electricity consumption. Most countries in Europe have plans for increasing their share of energy produced by wind power. The increased share of wind power in the electric power system makes it necessary to have grid-friendly interfaces between the wind turbines and the grid in order to maintain power quality.

In addition, power electronics is undergoing a fast evolution, mainly due to two factors. The first factor is the development of fast semiconductor valves, which are capable of switching fast and handling high powers. The second factor is the control area, where the introduction of the computer as a real-time controller has made it possible to adapt advanced and complex control algorithms. These factors together make it possible to have cost-effective and grid-friendly converters connected to the grid.

The thesis focuses on a forced-commutated voltage source converter connected to a grid in a wind energy application. When the first part of the project started up, the objective was to determine the optimal electrical system for a wind turbine, in terms of efficiency, cost and performance. Another goal was to investigate the voltage angle control method and its suitability for controlling a grid-connected voltage source converter in a wind turbine system. A simple, low-cost analog controller was used for the implementation. In efforts to increase the bandwidth of the system, a linear quadratic control method was considered.

The objectives of the second part of the project were to investigate the performance of the vector current control method when parameter variations, delay times and grid voltage distortion affect the vector current controller. To reduce the non-linearities from the valves and from the blanking time, a valve compensation function was implemented in the controller. The transformation angle detector, which synchronizes the voltage source converter to the grid voltage is essential to the vector current controller. One aim was to investigate different synchronization methods which could be implemented in the control-computer. Furthermore, the presumed high current bandwidth of the vector current controller could make it possible to implement extra applications. A higher power quality for the whole hybrid wind park can result in a lower total cost for the park.

This report consists of two parts. The first part contains a short discussion of wind turbine concepts, electrical systems used in wind turbines, control principles of voltage source converters and modulation techniques. Furthermore, the contributions and comments of the included papers are presented and the conclusions are stated.

The second part of the report consists of nine papers which are divided into four sections. The first section is an introduction to wind power, wind turbines, different electrical systems and hybrid wind parks. The second section investigates a voltage source converter connected to a grid using a voltage angle controller. In the third section, the vector current controller of the grid connected voltage source converter is investigated. Furthermore, four synchronization methods adapted for digital implementation are presented. One of the presented methods is a novel transformation angle detector based on a space vector filter. In the last section, the harmonics of the voltage source converter are investigated. Current harmonics attenuation at low and medium frequencies is compared for two grid filter types, the L-filter and the LCL-filter. Moreover, the influence of high voltage derivatives from fast switching valves is addressed.

2 Wind Turbine Configurations

The use of wind energy goes back far in history. Wind power plants have, for instance, been used as water pumps and as mills. One major difference between the earliest windmills and the new generation of wind turbines is that the mechanical transmission of power has been replaced by an electrical transmission. The oil crisis in the mid 1970s resulted in a new interest in wind energy. This attention has continued to grow as the demand for reduced polluting emissions has increased. The wind energy market today is small but growing rapidly.

2.1 Standard Fixed-speed Wind Turbine

The standard wind turbine plants of today use conventional horizontal-axis wind turbines. The turbine has two or three blades. In some designs, the blades can be pitched, to change the aerodynamic torque. The nacelle is placed on a high tower, in order to benefit from higher wind speeds high above ground. Furthermore, the low-speed turbine is connected to the generator via a gearbox, as shown in Fig. 1. The rotational speed of the generator is typically 1500 rpm and the turbine speed is 20 to 50 rpm. The induction machine is the most common generator type.

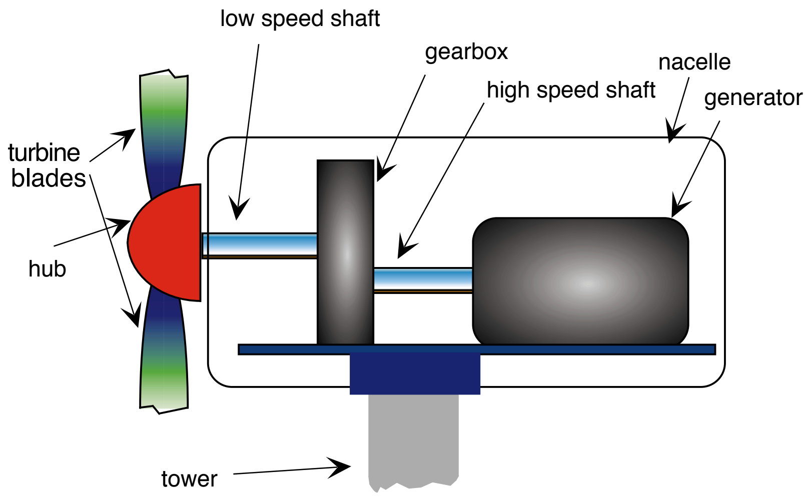

Figure 1: The parts of a wind turbine.

The kinetic power P_w of the air passing the swept turbine area A increases with the cube of the wind speed w, as

$$P_w = \frac{\rho A}{2} w^3 \tag{1}$$

where ρ is the density of air. At low wind speeds, the generated power is too low to be exploited. When the wind speed exceeds the cut-in wind speed, the wind turbine starts. The input power of the wind turbine must be reduced when the aerodynamic power becomes higher than the rated power of the wind turbine. Two common methods are used: The first method changes the pitch-angle of the blades. The second method is based on blades designed in such a way that they stall when wind speed exceeds a certain level. When wind speed reaches the cut-out speed, the wind turbine is shut down due to high mechanical loads. The cut-out speed is approximately 25 m/s. In Fig. 2 wind power and wind turbine power are shown as a function of wind speed.

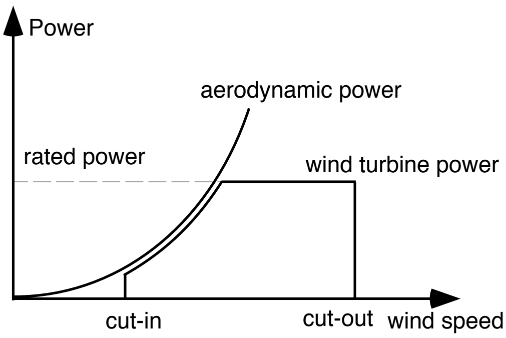

Figure 2: The ideal power curve of a wind turbine.

The probability density function of wind speed is usually described by a Weibull distribution [1]. Even if the wind turbine produces the rated power at the cut-out speed, the achieved energy capture is small at high wind speeds because the number of strong gale hours per year is few.

2.2 Variable-speed Wind Turbine

A wind turbine must run at a certain speed relative to the current wind-speed, defined by the optimal tip-speed ratio, in order to produce maximum power. For a fixed-speed concept, the efficiency will not be maximized. Losses depend on the exact design of the turbine and the wind variations at the site. An improvement of the single-speed turbine is the multiple-fixed-speed turbine (usually two speeds), provided by a generator with a changeable number of poles. An active pitch, which adjusts the pitch angle instantaneously to the wind speed, is an option to increase the energy capture. Unfortunately, the bandwidth of the active-pitch system is too small to utilize this advantage. A larger problem is wind power fluctuation at high wind speeds; the low bandwidth of the pitch control results in overloads. By introducing a variable-speed operation, it is possible to continuously adapt the rotational speed to the current wind speed, so that, ideally, the maximum obtainable power is continuously produced by the plant. Typically, this optimal mode is achieved for low to medium wind-speeds. The theoretical average efficiency of the electrical system can be increased by 5 % compared with a fixed-speed wind turbine [2]. If the plant is stall-regulated, the optimal turbine speed is proportional to the wind speed for wind speeds up to the rated speed. For higher wind speeds, turbine power is kept constant by means of a stall effect.

When using a variable-speed, stall-controlled wind turbine, the electrical system must be designed to manage a power overload. The maximum power from a stall-controlled wind turbine changes due to changes in the performance of the stall regulation. This increases the cost of the electrical system. When using both variable speed and pitch control, the electrical system can be designed to manage the rated power of the wind turbine.

3 Electrical Systems of Wind Turbines

The standard electrical system for a fixed-speed wind turbine is a squirrel-cage induction generator directly connected to a grid. To reduce the reactive power demand, a capacitor bank is installed to compensate for the no-load current of the generator. Furthermore, a thyristor-equipped, soft-starter is used to reduce the inrush current.

For variable-speed wind turbines, many different solutions of electrical systems are possible. In this report, only full-span, variable-speed systems are considered. The development of semiconductor components for use in the converters of the electrical system is progressing rapidly. The rated power of the valves increases, as a result, and the cost decreases. Furthermore, forced-commutated valves with shorter turn-on and turn-off times are introduced. In addition, the fast development of control computers has facilitated more advanced control algorithms.

A variable-speed electrical system has three main components. They are the generator, the rectifier and the inverter, shown in Fig. 3. The system can be split into two subsystems: inverter-grid and rectifier-generator. This helps when analysing one part of the system. Each sub-system has at least two different device alternatives.

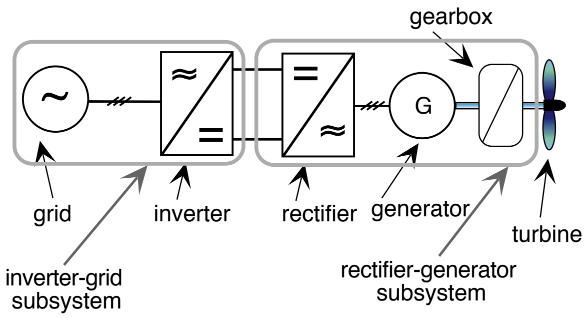

Figure 3: Overview of the electrical system for variable-speed system.

Two main types of generators are used: either the synchronous or the induction generator. The synchronous generator (SG) can use two methods of excitation: permanent magnets or field winding. A relatively new generator concept is the switched reluctance generator, which is cost-effective but, unfortunately, has a high torque ripple [3]. The common way is to use a field winding, because it has the advantage of controlling the three-phase voltage level; if the terminal voltage level is fixed, the produced reactive power can be controlled. In recent years, the costs of high performance permanent magnets have dropped and permanent magnet machines have become an interesting alternative compared with traditional machine types. When using permanent magnets, the electrical losses of the machine become smaller, which is positive. However, the voltage level is proportional to the speed. Due to the produced reactive power, the synchronous generator can be connected to a load-commutated rectifier, i.e., a diode rectifier or a thyristor rectifier. The voltage source converter (VSC), however, can be used as a rectifier. Observe that the controller of the VSC requires a minimum dc-link voltage relation to the generator voltage in order to operate properly.

The induction generator (IG) requires reactive power to operate. Consequently, the IG often uses the VSC, which produces reactive power. Another possibility is to use a diode rectifier or a thyristor rectifier together with capacitors, which produce the required reactive power. Unfortunately, reactive power changes with speed and if the capacitance value is not correct, the performance of the system will be low.

The inverter of the system is connected to the grid. Here, the grid-commutated inverter, also called the thyristor inverter, and the VSC can be used. The VSC requires a minimum dc-link voltage in order to operate, and in some cases a step-up converter (DC/DC) must be introduced to increase the voltage level for the VSC. The VSC can act both as a rectifier and as an inverter: the power direction is set by the controller.

To give an overview of the different electrical system combinations, Fig. 4 has been introduced. Observe that the combinations are primarily for systems which use a gearbox between the generator and the turbine.

A rather new concept is to use a directly-driven permanent magnet generator, which is directly connected to the turbine without a gearbox. Depending on the optimization of the rectifier-generator subsystem, the rated power can be increased by 50 % when using a VSC, instead of a diode rectifier or a thyristor inverter [4].

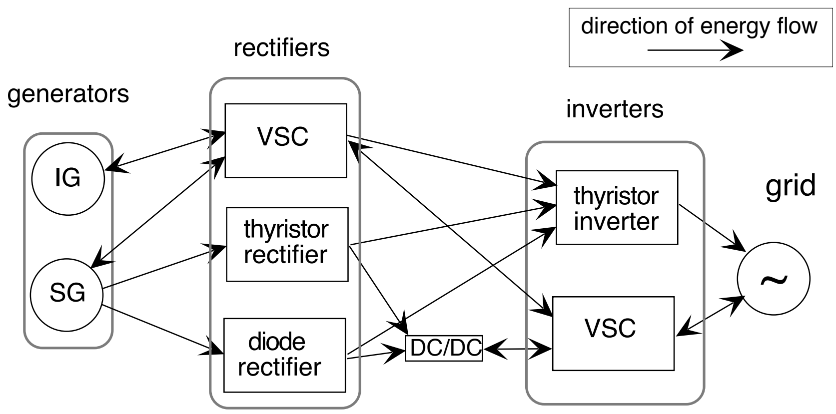

Figure 4: Diagram of different electrical system alternatives for variable speed.

4 Locations and Power Quality of Wind Turbines

Wind turbines are often located on coastal shores in rural areas, due to high wind speeds and sparse population. The grids connecting these areas are often weak, i.e., have a non-negligible, short-circuit impedance. This results in power quality problems when connecting wind turbines, which are not adapted to weak grids.

The most common electrical system of commercial wind turbines is the induction generator directly connected to the grid. A major drawback is that the reactive power flow and, thus, the grid voltage level cannot be controlled. Another drawback associated with a fixed-speed system is that the blade rotation causes power variations and, thereby, voltage fluctuations of a frequency of 1 to 2 Hz in the grid [5]. This fluctuation problem is not solved by using several turbines; on the contrary, if several identical wind turbines are installed in a wind park, the rotors can synchronize with each other and the power fluctuations will be superimposed in phase [6]. Furthermore, induction generator dynamics has resonance peaks around 10 Hz [7], where the sensitivity to flicker is high.

For the variable speed system, the inverter connected to the grid is a thyristor inverter or a VSC. Depending on the generator-rectifier sub-system, the thyristor inverter can be controlled in different ways. If a diode or thyristor rectifier and a synchronous generator are used, the dc-link voltage level will be proportional to the turbine speed, resulting in a reactive power transfer from the grid, and the reactive power will change with the active power delivered from the wind turbine, due to the varying firing angle of the thyristors. Another drawback of using a thyristor inverter is low-frequency current harmonics. If a thyristor inverter is connected to a weak grid, current harmonics will cause low-frequency voltage distortion from about 200 Hz to 1 kHz. Current harmonics can be reduced significantly by using tuned passive filters. Unfortunately, the filter size becomes large when removing low-frequency harmonics.

An alternative to a thyristor inverter is the VSC. If nothing else is mentioned, the valves of the voltage source converter are of the Insulated Gate Bipolar Transistor (IGBT) type. A VSC connected to the grid has several advantages in comparison with a thyristor inverter: The reactive power can be chosen freely, often set to zero to obtain the unity power factor. Grid currents become sinusoidal with no low-frequency harmonics, at least if a proper controller is used [8]. By using advanced control techniques, the power quality of the grid can be improved. Unfortunately a VSC has a few drawbacks: The efficiency is slightly lower in comparison with a thyristor inverter. Rated power has been a limit, but the fast development of valves has improved rated power. Also the voltage level has increased resulting in lower losses in other parts of the variable-speed electrical system.

The ability to control the turn-on and the turn-off characteristics of the IGBT has made it possible to parallel [9] and to series [10] connect several IGBT-valves, and, thus, increase the rated power of the converter. When comparing the cost of a thyristor inverter with a VSC, the thyristor inverter has a lower price, because it is a mature product and it has lower losses resulting in less cooling material. But when all the equipment around the inverters is included, the total system cost difference is levelled out.

In energy project plans for the future, it is understood that alternative energy is to be increased; the best way to increase the energy production from wind energy is to build large wind farms. To gain acceptance from the population, wind farms have been proposed to be installed offshore. This can lead to new solutions, such as high voltage direct current transmission of energy from the wind farm to a grid ashore.

5 Grid-connected VSC

The main purpose of this section is to introduce the reader to different aspects of a VSC connected to a grid. The main circuit configuration of the VSC is presented so the variables and their symbols can be defined and will be used henceforth. Furthermore, different types of grid filters and modulation techniques will be presented. Two control principles will be introduced, the voltage angle control and the vector current control principle. Finally, the modelling of the system will be described.

5.1 Main Circuit of VSC

A scheme of the main circuit of the VSC is shown in Fig. 5. The valves are of the IGBT-type. The VSC is connected to a symmetric three-phase load, which has the impedance $R + j\omega L$ and the emfs $e_1(t)$, $e_2(t)$ and $e_3(t)$. The neutral point of the star-connected load has the potential $v_0(t)$, due to a floating ground. The phase potentials of the VSC are denoted as $v_1(t)$, $v_2(t)$ and $v_3(t)$. The phase voltages of the VSC are denoted as $u_1(t)$, $u_2(t)$ and $u_3(t)$. The current flowing from the dc-link to the converter is denoted as $i_v(t)$, the dc-link current is denoted as $i_{dc}(t)$ and the dc-link voltage across the dc-link capacitor is denoted as $u_{dc}(t)$.

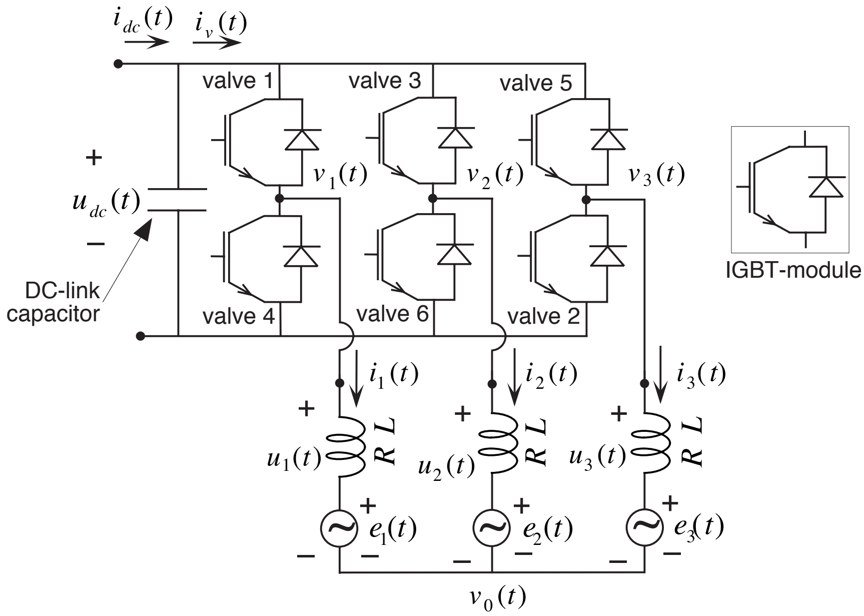

Figure 5: The main circuit of the VSC.

5.2 Grid Filters

When connecting a VSC to a grid, an inductor must be mounted between the VSC, which is operating as a stiff voltage source, and the grid, which also operates as a stiff voltage source [11]. The simplest and most common grid filter is the L-filter, which has three series connected inductors, one in each phase.

The LC-filter has the same series inductors, one in each phase, as the L-filter. In addition, the LC-filter has three parallel coupled capacitors. This filter type has often been investigated for systems which are used in autonomous grids as an uninterruptible power supply and in most investigations, the load consists of resistors, one in each phase [12]. When connecting a system with the LC-filter to a public grid, problems can occur due to resonances. The resonance frequency depends on the capacitor value of the filter and the inductance value of the grid, which varies over time. It is difficult to reduce the resonance, because resonance frequency changes with grid inductance and, in addition, the harmonic distortion spectrum of the grid changes with time.

The resonance problem can be reduced by using an LCL-filter [13]. The main advantages of using an LCL-filter are low grid current distortion and reactive power production. The resonance frequency can be determined almost independently of the grid configuration. The disadvantage is a more complicated system to control. The L-filter attenuation is a 20 dB/decade and the LCL-filter attenuation is a 60 dB/decade for frequencies over the resonance frequency of the filter. To improve the attenuation of the system when using the L-filter, a tuned shunt filter can be introduced which is tuned to the switching frequency of the VSC [14].

5.3 Modulation

One of the advantages of the VSC over the grid-commutated converter is low harmonic distortion at low frequencies, resulting in sinusoidal grid currents. This is due to the fact that by switching the valves properly only high-frequency harmonics remain. The research field of modulation techniques has been focused on reducing the number of switching instances per cycle while still obtaining low distortion due to the current ripple caused by the switching instances [15]. The simplest modulation technique is the six-pulse modulation, where each phase switches twice per cycle. The fundamental voltage amplitude becomes high but harmonics occur at low frequencies: 5th, 7th, 11th, 13th and so on. By introducing more switching instants, the current ripple will be reduced as well as the fundamental voltage amplitude. Depending on the rated power of the VSC, the switching frequency is reduced when the rated power is increased. For small adjustable-speed drive systems, the switching frequency can be as high as 20 kHz. For converters used in high power applications, the switching frequency is reduced down to approximately 1 kHz.

The most common modulation methods can be divided into two groups: either current control or voltage control. The current control method forces the valves to switch only when it is necessary to keep on tracking the reference of the current. This control principle is often called the current hysteresis control principle [16]. The second modulation type, voltage control, has as a common characteristic subcycles of constant time duration, a subcycle being defined as the total duration during which an active inverter leg assumes two consecutive switching states of opposite voltage polarity. Operation at subcycles of constant duration is reflected in the harmonic spectrum of the phase voltage by two dominating salient sidebands, centered around the switching frequency, and by additional frequency bands around integral multiples of the carrier [17]. The modulation type can be divided into two parts: a suboscillated pulse width modulation (PWM) and a space vector modulation, denoted by SVM. The latter modulation method is often used when microcontrollers are involved in the system. The suboscillation method is a classical modulation technique and employs individual modulators in each of the three phases. It is popular due to its simple implementation and is preferable when an analog system is used.

The input to a space vector modulator is the voltage reference vector in the αβ-frame, explained in Appendix A. The sampled input vector is then approximated by a time sequence of three well-defined switching state vectors. The ordinary three-phase voltage source converter has 8 switching vectors, also displayed in Appendix A. The modulation algorithm ensures that the time average of the switching state vectors over a sampling interval is equal to the reference vector [18]. Compared with the sub-oscillating PWM method, the SVM method can be modified to reduce the number of valve switchings during each sample interval or to change the switching valve pattern. The SVM has the following advantages: The reference voltage vector can be decomposed in a number of ways and the selected voltage vectors can be applied to different sequences. By controlling the SVM in a smart way, it is possible to reduce the switching frequency while still obtaining the same sample frequency as in the sub-oscillated PWM. This is an advantage when the rated power of the VSC is increased.

If the mid-point of the star-connected load is floating, a zero-sequence component can be added to all of the three phase reference voltages to extend the output voltage range of the converter by 15.5 % without losing the linearity from the reference voltage to the output voltage [19]. A triplen deadband PWM can be introduced to reduce the effective switching frequency, which reduces switching losses up to 33 % [20]. In this method, one leg of the converter is clamped for a certain period of time in each cycle, hence resulting in a deadband region in which no switching will occur.

5.4 Control of the VSC Connected to the Grid

In this report, two control principles are investigated for a VSC connected to a grid. They are the voltage angle control and the vector current control. Both controllers use the rotating *dq*-coordinate system, explained in Appendix A. Furthermore, only the L-filter is considered for use.

The simplified circuit of a grid-connected VSC is shown in Fig. 6. The phase voltages of the VSC are modelled as three voltage sources denoted as $u_1(t)$, $u_2(t)$ and $u_3(t)$. The equivalent series inductance and resistance of the L-filter are denoted as L_S and R_S, respectively.

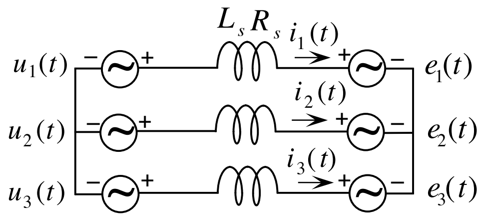

Figure 6: Schematic circuit of a grid-connected VSC, where the focus is on the L-filter.

The Kirchhoff voltage law can be applied to the circuit in Fig. 6. The equation becomes

$$\underline{u}^{(\alpha\beta)}(t) - R_s \underline{i}^{(\alpha\beta)}(t) - L_s \frac{d}{dt}\underline{i}^{(\alpha\beta)}(t) - \underline{e}^{(\alpha\beta)}(t) = 0 \quad (2)$$

In the *dq*-coordinate system, the equation becomes

$$\underline{u}^{(dq)}(t) - R_s \underline{i}^{(dq)}(t) - L_s \frac{d}{dt}\underline{i}^{(dq)}(t) - \mathrm{j}\omega_g L_s \underline{i}^{(dq)}(t) - \underline{e}^{(dq)}(t) = 0 \tag{3}$$

where the grid angular frequency is denoted as ω_g.

5.4.1 The Voltage Angle Controller

The voltage angle controller, also called the power angle controller, is a controller based on a system model in steady-state. By setting the derivative term in Eq. (3) to zero, the steady state expression becomes

$$\underline{u}^{(dq)}(t) - \underline{e}^{(dq)}(t) = \left(R_s + \mathrm{j}\omega_g L_s\right)\underline{i}^{(dq)}(t) \tag{4}$$

By controlling the phase displacement angle between the voltage vector of the VSC and the voltage vector of the grid and by controlling the magnitude of the voltage vector of the VSC, the active and reactive power can be controlled. The phase displacement angle and the relative voltage are denoted as $\theta(t)$ and $u_x(t)$, respectively. The relative voltage is used to control the magnitude of the voltage vector of the VSC and is defined as

$$u_x(t) = \frac{\left|\underline{u}_{(1)}(t)\right|}{\left|\underline{e}(t)\right|} \tag{5}$$

where $\left|\underline{u}_{(1)}(t)\right|$ is the magnitude of the fundamental voltage vector of the VSC. In Fig. 7, the grid and VSC voltage vectors are shown in the *dq*-coordinate system. To simplify the scheme, the resistance of the grid filter coil is set to zero. Furthermore, the phase displacement angle has been scaled up, to make it easier to understand the scheme. As shown in Fig.7, the current vector is perpendicular to the difference between the converter voltage vector and the grid voltage vector.

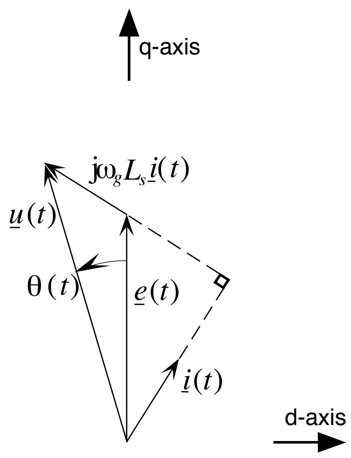

Figure 7: The principal scheme of voltage angle control.

To simplify the equations, the phase-to-phase voltage fundamental amplitudes of the VSC and the grid are denoted as U and E, respectively. If the grid and the VSC voltages are supposed to be distortion free and symmetric, the voltage vectors can be defined as

$$\underline{u}_{(1)}(t) = Ue^{\mathrm{j}\left(\theta(t)+\frac{\pi}{2}\right)} \tag{6}$$

$$\underline{e}(t) = Ee^{\mathrm{j}\frac{\pi}{2}} \tag{7}$$

The apparent power from the VSC to the grid is

$$\underline{s}(t) = \underline{u}_{(1)}(t)\bar{\underline{i}}(t) = \left(u_{d(1)}(t) + \mathrm{j}u_{q(1)}(t)\right)\left(i_d(t) - \mathrm{j}i_q(t)\right) \tag{8}$$

where the complexconjugate is denoted by a bar. By using Eqs.(4),(6),(7) and (8), the active power and the reactive power can be written as

$$P = \frac{UE}{\omega_g L_s}\theta \tag{9}$$

$$Q = \frac{E(E-U)}{\omega_g L_s} \tag{10}$$

where the resistance of the L-filter is neglected and the phase displacement angle is so small that the sine of the angle is approximately equal to the angle and the cosine of the angle is approximately equal to one. The active power is proportional to the phase displacement angle and the reactive power is proportional to the difference between the voltage amplitudes of the VSC and the grid. Investigated applications of converters using the voltage angle control are, for instance, high-voltage direct current (HVDC) converters [21,22] and static VAr compensators (SVCs) [23].

When using the voltage angle control of the VSC in a wind turbine application, the VSC connected to the grid is set to control the voltage level of the dc-link independent of the operating point of the generator-rectifier sub-system. The principle of the control scheme is shown in Fig. 8. This control has been implemented in a laboratory system [24]. The voltage vector angle $\theta_g(t)$ of the grid is obtained from an analog phase-locked loop (PLL) connected to one of the phase voltages of the grid. The amplitude of the grid voltage is obtained by low-pass (LP) filtering the rectified grid voltages through a three-phase diode rectifier. The goal of the dc-link voltage controller is to track the reference dc-link voltage $u^*_{dc}(t)$. The dc-link voltage is controlled by using a PI-controller, the input of which is the dc-link voltage error and the output is the phase displacement angle $\theta(t)$. The relative voltage $u_x(t)$ is determined by the reactive power controller, which has the reactive power reference $Q^*(t)$ and the grid voltage amplitude as inputs. The inputs to the PWM-unit are: The total voltage vector angle of the VSC, which is the sum of the phase displacement angle $\theta(t)$ and the grid voltage vector angle $\theta_g(t)$; the dc-link voltage $u_{dc}(t)$ and the relative voltage $u_x(t)$.

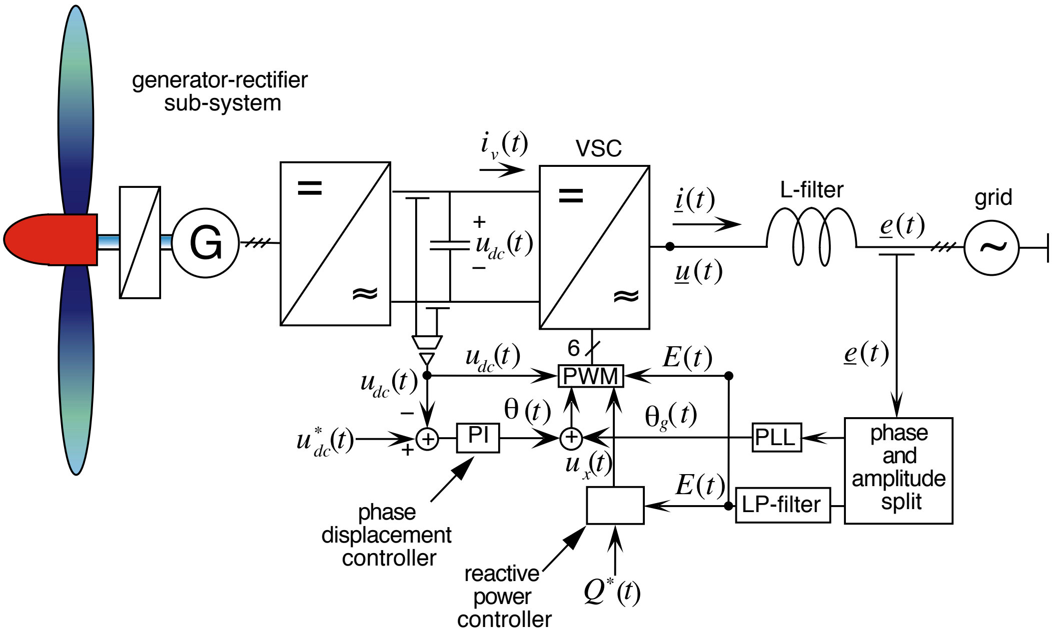

Figure 8: The principal control scheme of the voltage angle control in a variable-speed wind turbine application.

The voltage angle control is simple to implement in an analog controller or a micro-controller. However, the bandwidth of the system is low, since the controller is based on a steady-state model. The bandwidth required for controlling the wind turbine is low due to the large inertia of the turbine, which acts as an LP-filter. Furthermore, the power above 1 Hz in the wind power spectrum is small. However, it is important that the control system can damp drive train resonances actively. To do that, the bandwidth of the system must be around 10 Hz. Often the reactive power demand is set to zero to obtain a high power factor. But, if the grid is weak, the reactive power can be used to control the voltage level of the grid.

When using the voltage angle control principle, it is easy to implement an efficient PWM-generator, where the pulse pattern has been calculated off-line and stored in an EPROM. This is important if the rated power is high and the switching losses must be low. As described above, the voltage angle control principle is simple and a few simple control blocks are needed. Furthermore, grid phase currents must not to be measured to perform the control principle. The controller implementation can be made inexpensive due to the low bandwidth requirement. This indicates that the control system should be used in plants where the relative controller cost is high, i.e., low-rated power plants.

5.4.2 The Vector Current Controller

The basic principle of the vector current controlled grid-connected VSC is to control the instantaneous active and reactive grid currents independently of each other and with a high bandwidth. In this thesis, the vector current controller is implemented in a computer, the control functions are discrete and the inputs and outputs to the controller are sampled at a constant sample frequency. In the laboratory system, the sample frequency is equal to the switching frequency.

The currents and the voltages of the grid are transformed to the rotating *dq*-coordinate system. By this operation, the fundamental current and voltage components become dc-quantities and PI-controllers can be used to reduce steady-state errors. The components of the reference voltage out from the regulator are transformed back to three-phase quantities and used as inputs to the PWM function. In Fig. 9, the principal block diagram of the system and the controller are shown.

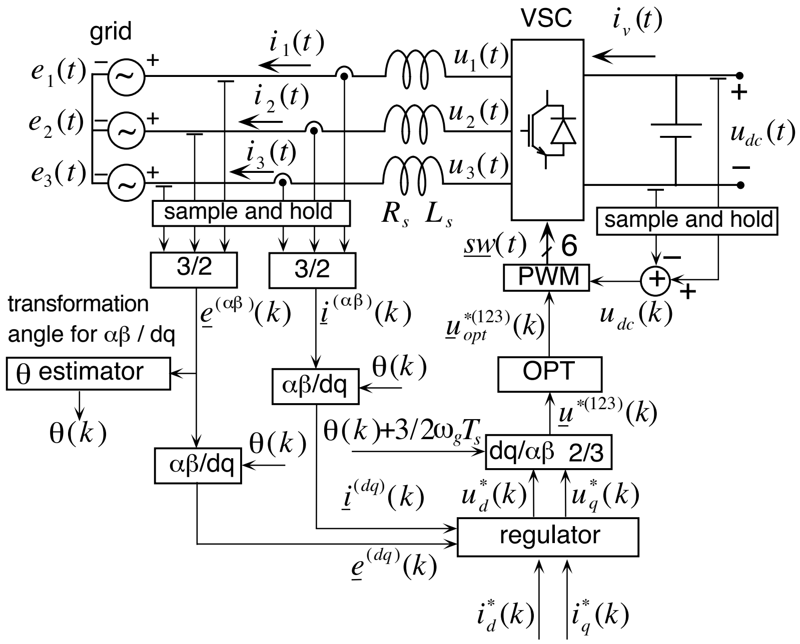

Figure 9: Principal block diagram of vector current controller.

To obtain a high bandwidth, the total system must be well-known including the influences of non-ideal components, the grid filters and the filters in the signal paths. The following items are important:

- Correct sampling instances. If the phase currents are sampled exactly at the top and bottom of the triangular wave used in the sub-oscillated PWM, the ripple of the current is zero. An error in the measured current occurs if the sample instance is delayed a few microseconds, then the error will increase if the current ripple increases.

- Overmodulation. If high gains are used, the reference voltage vector from the vector current controller will be large when trying to realize demanded current steps, and the PWM cannot realize the demanded voltage vector and an overmodulation occurs. This results in uncontrolled phase currents.

- One-sample delay in the current controller. If a discrete sampled control system is used, a delay time of one sample will occur due to the calculation time of the control-computer. If a high bandwidth is required, for instance dead-beat, high gains must be used in the current controller and the influence of the delay time must be compensated in the controller to eliminate oscillations. When not compensating for the delay time, the gain must be decreased [25].

- Valve non-linearities. In a real converter, the on-state voltage drop and the resistance of the valves of the converter influence the system negatively, such as performance of the current control and low-frequency current harmonics. A compensation function can be implemented if the non-linearities are known [26].

- Non-ideal PWM. To protect from short circuits in the phase-legs, a blanking time is introduced. The blanking time is the time between the turn-off of a valve in the phase-leg and the turn-on of the second valve in the phase-leg. This blanking time reduces the mean voltage under the sample period [26].

- Grid voltage distortion. Grid voltage distortion affects the current controller. There is a coupling between the grid voltage harmonics and current out from the converter.

- Synchronization of the transformation angle to the grid voltage. It is important that the synchronization operates effectively even if the grid has a poor power quality.

The obtained high bandwidth can be used in high-performance applications such as active filtering [27]. A cost effective solution can be obtained by reducing the component costs such as the dc-side capacitor and the grid filter; it is still possible to achieve a high power quality for applications such as rectifiers in drive systems or inverters connected to the grid in wind turbine plants.

5.5 Modelling of Control-circuit and VSC Connected to a Grid

When analysing the VSC system, a model must be created. The model should include the grid, the grid filter, the dc-link and the VSC and its controller. Two model objects are in focus: modelling the system to obtain a simulation model and creating a small-signal model of the system.

To determine proper control gains for the control loop design of the VSC system, a small-signal analysis is performed around an operating point. The small-signal model is obtained by linearizing the large-signal model of the system, which is often linear except for the discontinuity due to the pulse width modulated valves. By assuming the pulse width modulated voltage of the converter to be a constant voltage during the sample period, a linear state equation can be formed, where the states are piecewise constant under the sample period. This assumption is valid when changes in the reference voltage are slow in comparison with the switching intervals of the converter. Two common averaging methods are: the state-space averaging [28,29] and the average switch model [30].

For dc-dc converters, model accuracy can be increased by using the transient behavioural model (TBM). In this model, the first harmonic tone is added to the mean voltage during the sample period, resulting in increased performance [30]. Often, the VSC system is modelled on the rotating *dq*-coordinate system and the coordinate transformations and the valves are assumed to be ideal. For this situation, the space vector averaging method should be used, because the correct mean voltage vector is obtained during the sample period. The average switch model averages each phase individually, and if the voltages are wanted in the *dq*-coordinate system, coordinate transformations must be performed. If the ratio between the sample frequency and the grid frequency is small, the coordinate transformation together with the pulse width modulated signal can introduce errors [31].

Transfer functions of the Laplace-transformed system work well for single-input single-output (SISO) systems. But if multiple-input multiple-output (MIMO) systems are considered, the transfer function matrices become awkward to use. Furthermore, if the analysed system has time delays, which are modelled as $\exp(-sT)$, the system must be linearized by using, e.g., the Padé approximation. Unfortunately, the polynomial degree will increase significantly. For VSC systems using discrete controllers, the discrete state equation is preferable and an one-sample delayed variable results in only one more variable in the state vector. To obtain the discrete closed-loop state equation, the grid voltage and the L-filter must be discretized. A major advantage of using discrete models in comparison with continuous models, including the switching instances, is the reduced simulation time.

6 Contributions, Comments, Conclusions and Future Research

The field of power electronics has been growing rapidly since the evolution of semiconductors. Computers and semiconductor valves increase their performance at high speed. As a result of this development, the high-performance devices of yesterday have become today's mediocre devices and, of course, published articles have also become out-of-date.

The outline of this chapter is as follows. In Section 6.1, the contributions and comments of the included papers are given. In Section 6.2, the author's conclusions are stated. Lastly, suggestions for future research are given.

6.1 Contributions and Comments of Included Papers

Paper 1A

Paper 1A acts as an introduction and also gives an overview of different electrical systems for variable-speed wind turbines. The proposed electrical system to be used in a variable-speed wind turbine consists of a synchronous generator, a diode rectifier and a grid-connected thyristor inverter, if the grid is strong. If the grid is weak, an IGBT chopper together with a forced-commutated voltage source converter is recommended, instead of the thyristor inverter. The background material about losses and converter prices originates from a study made in 1993. Due to the fast development of components and price changes for the devices, the cost results given in the paper are not valid any more. The losses in the grid filter are roughly estimated. New types of slowly-rotating permanent-magnet generators have been introduced after the publication of the paper; they result in a system without a gearbox and are of great interest today. If the new type of generator is used, a forced-commutated rectifier should be used to increase the efficiency and the rated power of the system, and the proposed IGBT chopper can be terminated.

Paper 1B

Paper 1B investigates a hybrid wind park, which is connected to a weak grid. The amplitude of the grid voltage at the point of common connection is focussed on. A grid-connected voltage source converter injects reactive power into the grid and affects the voltage level. The size of the voltage source converter for different electrical system combinations is analysed. It turns out that the increase in the rated power of the voltage source converter, when both delivering active power from the wind turbine and injecting reactive power to the grid, is moderate in comparison with only delivering active power. The results depend strongly on the short-circuit impedance ratio and the short-circuit ratio of the grid. In the paper, all converters and their control systems are assumed to be ideal.

Paper 1C

Paper 1C is an extension of the work presented in Paper 1B. The increase in the rated size of the voltage source converter is investigated for different combinations of electrical systems in the hybrid wind park. Furthermore, the effect of cancelling reactive power as well as harmonic currents from the hybrid wind park on the rated size of the voltage source converter is presented. The grid is assumed to have an infinite short-circuit power and the voltage source converter together with its control system is supposed to operate ideally. Only harmonics up to the 13th order are considered, which is partially due to the moderate sampling frequency of the inverter. When using the voltage source converter simultaneously as an active power transmitter, a reactive power compensator and as a current harmonic canceller, the switching frequency should be moderate to keep down the losses in the converter. This results in a low current bandwidth and also restricts the highest frequency of the harmonics which can be cancelled. It turns out that the rating of the voltage source converter only needs to be increased moderately to fulfil the requirement for high power quality at the point of common connection.

Paper 2A

Paper 2A introduces an electrical system in a variable-speed wind turbine, in which the voltage source converter uses the voltage angle control principle to track the reference voltage of the dc-link independently of the delivered power from the generator-rectifier subsystem. An analog controller is used and, in the frequency analysis, the dc-link voltage fluctuation is neglected when calculating the current in the dc-link. The result of the investigation is that a voltage angle control can be used in a wind power application. Furthermore, the bandwidth of the inverter system is around 20 to 30 Hz depending on the parameter values of the system.

Paper 2B

Paper 2B introduces the linear quadratic (LQ) control method into the voltage angle controlled voltage source converter in a wind energy application. The LQ-control method is used to increase the bandwidth of the voltage angle controlled converter system; simulations show that the control method operates as expected. An analog implementation of the LQ-controller is used, since the paper is a continuation of Paper 2A, in which an analog controller was used. The system is non-linear and to get a high-performance controller, gain scheduling is used. The phase displacement angle is used to determine which gain should be used. One disadvantage of using the LQ-controller is the low attenuation of noise at frequencies near the model excitation frequencies. Therefore, an extended Kalman estimator was introduced to decrease the influence of current harmonics near the switching frequency. If a discrete LQ-controller had been used instead of the analog one, and if a proper sampling of the variables had been done, the performance of the system would probably have been improved.

Paper 3A

In Paper 3A, a grid-connected voltage source converter using a discrete vector current controller is investigated. A discrete state equation model of the grid-connected voltage source converter and its controller is derived both for a "fast computer" and for a one-sample delayed controller. The used controller inductance and resistance parameters of the grid filter inductor are changed to simulate an incorrect controller tuning. The mistuned controller is used in the model of the system for predicting responses of grid voltage harmonics. It is assumed that the sampling of the system variables, as well as the valves and the pulse width modulation, are ideal. The delay time of one sample in the discrete controller, due to the calculation time of the computer, results in a higher cross-coupling gain from the reference *d*- and *q*-currents to the *q*- and *d*-currents. Moreover the phase lag becomes larger. The delay time results in a coupling between grid voltage harmonics and the three-phase currents of the converter, and the gain increases with frequency. The investigated errors in the controller parameters show that the vector current controller can handle inductance variations of ± 25 % and resistance variations of ± 50 %. To increase reference current tracking capacity, a modified delay time compensator, based on the Smith predictor, could be used instead of the one presented in the paper, which cannot handle overmodulations properly.

Paper 3B

In Paper 3B different synchronization methods for grid-connected voltage source converters are proposed. The methods are adapted to be used in digital controllers. A novel synchronization method based on a space vector filter (SVF), which properly handles phase jumps in grid voltage, is presented. In addition, an extended variant of the SVF is presented; this variant handles both phase jumps in grid voltage and grid frequency changes. This method has an even higher performance than the extended Kalman filter method, in spite of the smaller number of calculations that must be performed. In the paper, the three-phase grid voltage is assumed to be symmetric.

Paper 3C

Paper 3C extends the work of Paper 3A to involve experimental results of a vector current controlled VSC connected to the grid. The focus is on the frequency response from the reference current to the current in the *dq*-frame at an operating point. The grid filter inductor influences the current controller due to high losses when the frequency is increased. A valve compensation function is introduced to reduce the influence of the non-linearites of the valves and the blanking time of the pulse width modulation. In this paper, the influence of the valve compensation function and the integration term in the current controller are analysed in a small-signal scheme. The integration term does not influence the small-signal performance. However, the valve compensation function improves the performance of the current controller. The influences of the non-perfect sampling due to delays, the accuracy in the measurements and grid voltage harmonics are not considered when comparing the measurement results with the analytical ones.

Paper 4

One disadvantage of voltage source converters is generated voltage harmonics due to the valve switching of the converter. When using the sub-oscillated pulse width modulation, the harmonics occur around the switching frequency and multiples of it. The voltage harmonics from the converter result in grid current harmonics depending on the grid filter. Paper 4 focuses on low- and medium-frequency harmonics and in harmonic distortion above 100 kHz. The L-filter is compared with the third-order LCL-filter; the outcome is that the LCL-filter is proposed due to the better attenuation of low- and medium-frequency current harmonics. The fast-switched valves result in high voltage derivatives. This produces insulation stresses in the transformer or the grid filter connected to the converter. If long cables are used, the insulation stresses are further increased due to reflections. In the experiments, large reflections occurred at a cable length of 20 meters.

6.2 Conclusions

In the thesis, different types of electrical system configurations for variable-speed wind turbines have been investigated. Furthermore, different control principles used on the voltage source converter connected to a three-phase grid have been focused on.

The electrical system which is recommended consists of a voltage source converter connected to the grid if high power quality is needed. The alternative is a thyristor inverter. The directly-driven permanent magnet generator with a voltage source converter used as a rectifier has become a promising alternative to the ordinary synchronous generator and the diode rectifier. The simple and low-cost voltage angle control method has been shown to manage a wind turbine application. The extended version of the voltage angle control, which uses a linear quadratic controller, has a higher performance and operates as expected.

The vector current controlled voltage source converter has a high bandwidth in comparison with the voltage angle control method. The controller handles parameter variations well. The valve compensation function decreases the current error in steady-state, and frequency responses show that the small-signal performance increases. The L-filter inductors applied, decrease the performance at high frequencies. A novel synchronization method based on a space vector filter handles both phase jumps in the grid and grid frequency changes.

To increase the power quality in a hybrid wind park, the voltage source inverter is proposed to act both as a reactive power compensator and as an active filter, at the same time delivering active power into the grid. It is shown that the rated power of the voltage source converter increases moderately in comparison with delivering only active power.

6.3 Future Research

The performance of control computers will continue to grow. This emphasizes the need for implementing better control functions and models, while still obtaining real-time control. Moreover, the performance of valves will increase continuously. A large step will be taken when transistor valves using silicon-carbide become available on the market. The performance of converters will increase, and new applications for power electronic devices will be introduced.

A proper continuation of this work is to apply an efficient control algorithm to restrain the influence of poor power quality. In other words, it should be possible to design a controller to suppress low-frequency voltage harmonics, swells, dips, unbalance as well as phase jumps due to short-circuits in the surroundings.

When the rated power of the converter increases, the short-circuit power ratio between the short-circuit power of the grid and the rated power of the converter connected to the grid will decrease. If a high performance is to be obtained, the shrinking short circuit ratio must be regarded. By improving the algorithms of the vector current controller and the converter synchronization to the grid, a high bandwidth can be obtained for the VSC connected to a weak grid.

7 References

[1] G. L. Johnson *Wind Energy Systems*. Prentice-Hall, Inc., Englewood Cliffs, New Jersey, 1985. 360 p.

[2] A. Grauers, "Higher Electrical Efficiency with Variable Speed," *European Community Wind Energy Conference*, Lübeck-Travemünde, Germany, 8-12 March 1993, pp. 656-658.

[3] R. Cardenas, W. F. Ray, G. M. Asher, "Transputer-Based Control of a Switched Reluctance Generator for Wind Energy Application," *6th European Conference on Power Electronics and Applications (EPE'95)*, Sevilla, Spain, 19-21 September 1995. Proceedings, Vol. 3, pp. 539-544.

[4] A. Grauers, "Design of Direct-driven Permanent-magnet Generators for Wind Turbines," Doctoral Thesis, Technical Report No. 292, Chalmers University of Technology, Göteborg, Sweden, 1996.

[5] F. Santjer, G. Gerdes, "Netzrückwirkungen, verursacht durch den Betrieb von Windkraftanlagen am Netz," *DEWI Magazin*, August 1994, pp. 35-41.

[6] A. Stampa, F. Santjer, "Synchronisation von netzgekoppelten Windenergie anlagen in einem Windpark," *DEWI Magazin*, August 1995, pp. 80-86.

[7] T. Thiringer, "Measurement and Modelling of Low-frequency Disturbances in Induction Machines," Doctoral Thesis, Technical Report No. 293, Chalmers University of Technology, Göteborg, Sweden, 1996.

[8] J. Berding, G. Santjer, "Netzrückwirkungen von Windenergieanlagen in Windparks," *DEWI Magazin,* Nr. 9, August 1996, pp. 30-36.

[9] P. Hofer, N. Karrer, C. Gerster, "Paralleling Intelligent IGBT Power Modules with Active Gate-Controlled Current Balancing," *Power Electronics Specialists Conference (PESC'96)*, Baveno, Italy, 23-27 June, 1996, pp. 1312-1316.

[10] C. Gerster, P. Hofer, N. Karrer, "Gate-Control Strategies for Snubberless Operation of Series Connected IGBTs," *Power Electronics Specialists Conference (PESC'96)*, Baveno, Italy, 23-27 June, 1996, pp. 1739-1742.

[11] K. Thorborg, *Power Electronics — in Theory and Practice*. Lund, Sweden, Studentlitteratur, 1993.

[12] Y. Ito, S. Kawauchi, "Microprocessor-based Robust Digital Control for UPS with Three-Phase PWM Inverter," *IEEE Transactions on Power Electronics*, Vol. 10, No. 2, March 1995, pp. 196-204.

[13] A. Draou, Y. Sato, T. Kataoka, "A New State Feedback-based Transient Control of PWM AC to DC Voltage Type Converters," *IEEE Transactions on Power Electronics*, Vol. 10, No. 6, March 1995, pp. 716-724.

[14] S. Bhattacharya, T. M. Frank, D. M. Divan, B. Banerjee, "Parallel Active Filter System Implementation and Design Issues for Utility Interface of Adjustable Speed

Drive Systems," *IEEE Industry Applications Society 31st IAS Annual Meeting*, San Diego, California, USA, October 6-10,1996, Vol. 2, pp 1032-1039.

[15] J. Holtz, "Pulsewidth Modulation for Electronic Power Conversion," *Proceedings of the IEEE*, Vol. 82, No. 8, August 1994, pp. 1194-1214.

[16] L. J. Borle, C. V. Nayar, "Zero Average Current Error Controlled Power Flow for AC-DC Power Converters," *IEEE Transactions on Power Electronics*, Vol. 10, No. 6, November 1995, pp. 725-732.

[17] K. Taniguchi, Y. Ogino, H. Irie, "PWM Technique for Power MOSFET Inverter," *IEEE Transactions on Power Electronics*, Vol. 3, No. 3, July 1988.

[18] J. Holtz, E. Bube, "Field-Oriented Asynchronous Pulse-Width Modulation for High-Performance AC Machine Drives Operating at Low Switching Frequency," *IEEE Transactions on Industry Applications*, Vol. 27, No. 3, May/June 1991, pp 574-581.

[19] V. Kaura, V. Blasko, "Operation of a Voltage Source Converter at Increased Utility Voltage," *IEEE Transactions on Power Electronics*, Vol. 12, No. 1, January 1997, pp. 132-137.

[20] M. F. M. Mohd Siam, B. W. Williams, S. J. Finney, "Improved Active Power Filter With Triplen Deadband PWM," *Power Electronics Specialists Conference (PESC'96)*, Baveno, Italy, 23-27 June, 1996, pp. 1899-1905.

[21] Å. Ekström, "Calculation of Transfer Functions for a Forced-commutated Voltage-source Converter," *Power Electronics Specialists Conference (PESC'91)*, Boston, USA, June, 1991, pp. 314-322.

[22] B. T. Ooi, X. Wang, "Voltage Angle Lock Loop Control of the Boost Type PWM Converter for HVDC Application," *IEEE Transactions on Power Electronics*, Vol. 5, No. 2, April 1990, pp. 229-234.

[23] G. Joos, L. Morán, P. Ziogas, "Performance Analysis of a PWM Inverter VAR Compensator," *IEEE Transactions on Power Electronics*, Vol. 6, No. 3, July 1991, pp. 380-391.

[24] J. Svensson, "Power Angle Control of Grid-connected Voltage Source Converter in a Wind Energy Application," Technical Report No. 218L, Chalmers University of Technology, Göteborg, Sweden, 1995.

[25] V. Blasko, V. Kaura, "A New Mathematical Model and Control of a Three-phase AC-DC Voltage Source Converter," *IEEE Transactions on Power Electronics*, Vol. 12, No. 1, Januariy 1997, pp. 116-123.

[26] J. K. Pedersen, F. Blaabjerg, J. W. Jensen, P. Thogersen, "An Ideal PWM-VSI Inverter with Feedforward and Feedback Compensation," *5th European Conference on Power Electronics and Applications (EPE'93),* Brighton, England, 13-16 September 1993, pp. 501-507.

[27] H. Akagi, "Trends in Active Power Line Conditioner," *IEEE Transactions on Power Electronics*, Vol. 9, No. 3, May 1994, pp. 263-268.

[28] S. R. Sanders, J. M. Noworolski, X. Z. Liu, G. C. Verghese, "Generalized Averaging Method for Power Conversion Circuits," *IEEE Transactions on Power Electronics*, Vol. 6, No. 2, April 1991, pp. 251-259.

[29] B. Lehman, R. M. Bass, "Extensions of Averaging Theory for Power Electronics System," *IEEE Transactions on Power Electronics*, Vol. 11, No. 4, July 1996, pp. 542-553.

[30] R. Kagalwala, S. S. Venkata, P. O. Lauritzen, A. Sundaram, R. Adapa, "A Transient Behavioral Model (TBM) for Power Converters," *IEEE 5th Workshop on Computers in Power Electronics, Portland*, USA, August 11-14, 1996, pp. 18-24.

[31] S. Hiti, D. Boroyevich, "Small-signal Modeling of Three-phase PWM Modulators," *Power Electronics Specialists Conference (PESC'96)*, Baveno, Italy, 23-27 June, 1996, pp. 550-555.

Appendix A

Transformations for Three-phase Systems

The transformations in this appendix are used when analysing three-phase machines and three-phase converters dynamically [1]. The transformations ensure power invariance.

A.1 Transformations between Three-phase and αβ-system

The three phase quantities $x_1(t)$, $x_2(t)$ and $x_3(t)$ can be transformed into two vectors, positive- and negative-phase sequence vectors, in a complex reference frame, called αβ-frame

$$\underline{x}_p(t) = x_{p\alpha}(t) + \mathrm{j}x_{p\beta}(t) = \sqrt{\frac{2}{3}}\left[x_1(t) + \mathrm{e}^{\mathrm{j}\frac{2\pi}{3}}x_2(t) + \mathrm{e}^{\mathrm{j}\frac{4\pi}{3}}x_3(t)\right] \tag{A.1}$$

and

$$\underline{x}_n(t) = x_{n\alpha}(t) + \mathrm{j}x_{n\beta}(t) = \sqrt{\frac{2}{3}}\left[x_1(t) + \mathrm{e}^{\mathrm{j}\frac{4\pi}{3}}x_2(t) + \mathrm{e}^{\mathrm{j}\frac{2\pi}{3}}x_3(t)\right] \tag{A.2}$$

where the sum of the three-phase quantities will be zero when no conductor is connected to the mid-point of the three-phase system, i.e.,

$$x_1(t) + x_2(t) + x_3(t) = 0 \tag{A.3}$$

A.1.1 Positive-Phase Sequence

The normal condition of a grid is to have positive-phase sequence vectors and no negative-phase sequence vectors. Hereby, a vector in the αβ-frame without the subscript *p* denotes a positive sequence vector. Equation (A.1) can now be expressed as a matrix equation

$$\begin{bmatrix} s_\alpha(t) \\ s_\beta(t) \end{bmatrix} = \mathbf{C_{23}} \begin{bmatrix} s_1(t) \\ s_2(t) \\ s_3(t) \end{bmatrix} \tag{A.4}$$

and the inverse becomes

$$\begin{bmatrix} s_1(t) \\ s_2(t) \\ s_3(t) \end{bmatrix} = \mathbf{C_{32}} \begin{bmatrix} s_\alpha(t) \\ s_\beta(t) \end{bmatrix} \tag{A.5}$$

where

$$\mathbf{C_{23}} = \begin{bmatrix} \sqrt{\frac{3}{2}} & 0 & 0 \\ 0 & \frac{1}{\sqrt{2}} & -\frac{1}{\sqrt{2}} \end{bmatrix} \qquad \mathbf{C_{32}} = \begin{bmatrix} \sqrt{\frac{2}{3}} & 0 \\ -\frac{1}{\sqrt{6}} & \frac{1}{\sqrt{2}} \\ -\frac{1}{\sqrt{6}} & -\frac{1}{\sqrt{2}} \end{bmatrix}$$

A.2 Currents and Voltages of Voltage Source Converter

The three-phase voltages of the voltage source converter can be represented in state-space vectors by the phase voltages $u_1(t)$, $u_2(t)$ and $u_3(t)$. The voltage vector in the complex αβ-frame becomes

$$\underline{u}(t) = u_\alpha(t) + \mathrm{j}u_\beta(t) \tag{A.6}$$

From now on, the valves of the voltage source converter are replaced by ideal switches. The switches sw_1, sw_2 and sw_3 of the converter can have a total of eight different combinations. For each state of the total number of combinations of switches, a state-space vector $\underline{sw}$ can be written as

$$\underline{sw}(t) = \sqrt{\frac{2}{3}}\left(sw_1(t) + \mathrm{e}^{\mathrm{j}\frac{2\pi}{3}} sw_2(t) + \mathrm{e}^{\mathrm{j}\frac{4\pi}{3}} sw_3(t)\right) = sw_\alpha(t) + \mathrm{j}sw_\beta(t) \tag{A.7}$$

In Table A.1, the eight different switch combinations and the state-space vectors of the switch values are shown. In Fig. A.1, the different switch states are presented in the form of state-space vectors.

TABLE A.1
SWITCH COMBINATIONS

sw_1	sw_2	sw_3	$\underline{sw}$
1	−1	−1	$\sqrt{\frac{8}{3}}\mathrm{e}^{\mathrm{j}\frac{0\pi}{3}}$
1	1	−1	$\sqrt{\frac{8}{3}}\mathrm{e}^{\mathrm{j}\frac{1\pi}{3}}$
−1	1	−1	$\sqrt{\frac{8}{3}}\mathrm{e}^{\mathrm{j}\frac{2\pi}{3}}$
−1	1	1	$\sqrt{\frac{8}{3}}\mathrm{e}^{\mathrm{j}\frac{3\pi}{3}}$
−1	−1	1	$\sqrt{\frac{8}{3}}\mathrm{e}^{\mathrm{j}\frac{4\pi}{3}}$
1	−1	1	$\sqrt{\frac{8}{3}}\mathrm{e}^{\mathrm{j}\frac{5\pi}{3}}$
1	1	1	0
−1	−1	−1	0

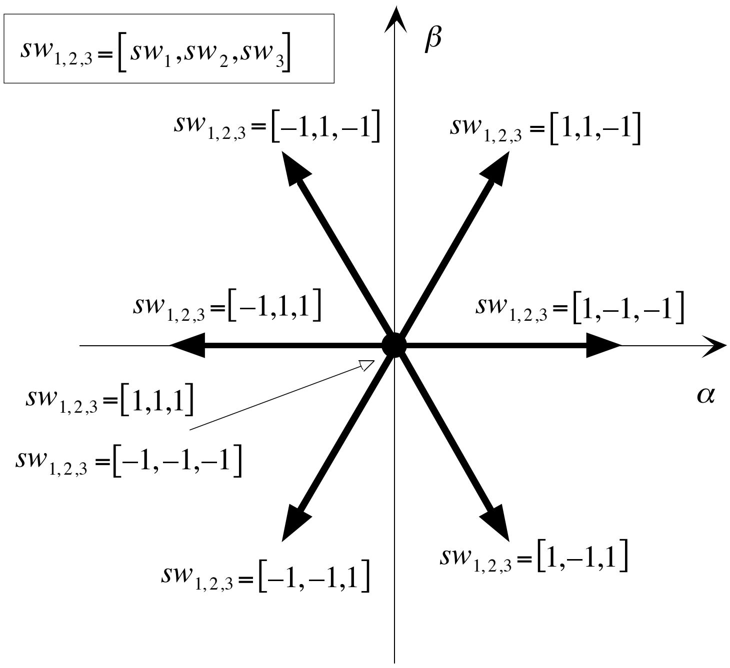

Figure A.1: State-space vector representation of the voltage vectors for the voltage source converter.

The output voltages of the voltage source converter can now be written as a state-space vector

$$\underline{u}(t) = \frac{u_{dc}}{2}\underline{sw}(t) \tag{A.8}$$

In a similar fashion, the three phase currents $i_1(t)$, $i_2(t)$ and $i_3(t)$ can be expressed as a state-space vector

$$\underline{i}(t) = \sqrt{\frac{2}{3}}\left(i_1(t) + e^{j\frac{2\pi}{3}} i_2(t) + e^{j\frac{4\pi}{3}} i_3(t)\right) = i_\alpha(t) + j i_\beta(t) \tag{A.9}$$

The sum of the three-phase currents is always zero. The DC-link current $i_V(t)$ between the dc-link capacitor and the voltage source converter can be written as

$$i_V(t) = sw_1(t)i_1(t) + sw_2(t)i_2(t) + sw_3(t)i_3(t) = \mathrm{Re}\left[\underline{i}(t)\,\mathrm{conj}(\underline{sw}(t))\right] \tag{A.10}$$

A.3 The Connection between the αβ– and the *dq*-system

Let the vectors $\underline{v}(t)$ and $\underline{w}(t)$ rotate with the angular frequency ω and ω_g in the αβ-frame, respectively. The vector $\underline{v}(t)$ becomes a fixed vector in the *dq*-frame if the vector $\underline{w}(t)$ forms the *d*-axis in the *dq*-frame and the angular frequencies ω and ω_g are equal, as illustrated in Fig. A.2.

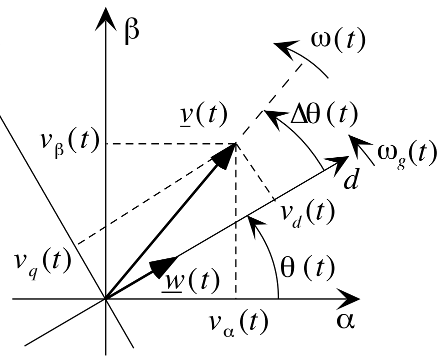

Figure A.2: The relation between the αβ-frame and the dq-frame.

The angles $\theta(t)$ and $\Delta\theta(t)$ in Fig. A.2 are given by

$$\theta(t) = \int_0^t \omega_g(\tau)d\tau \tag{A.11}$$

$$\Delta\theta(t) = \int_0^t \left[\omega(\tau) - \omega_g(\tau)\right]d\tau \tag{A.12}$$

The components in the *dq*-frame can be determined from Fig. A.2. The transformation equation from the αβ-frame to the *dq*-frame becomes, in matrix form

$$\begin{bmatrix} v_d(t) \\ v_q(t) \end{bmatrix} = \mathbf{R}(-\theta(t)) \begin{bmatrix} v_\alpha(t) \\ v_\beta(t) \end{bmatrix} \tag{A.13}$$

and the inverse becomes

$$\begin{bmatrix} v_\alpha(t) \\ v_\beta(t) \end{bmatrix} = \mathbf{R}(\theta(t)) \begin{bmatrix} v_d(t) \\ v_q(t) \end{bmatrix} \tag{A.14}$$

where the projection matrix is

$$\mathbf{R}(\theta) = \begin{bmatrix} \cos(\theta) & -\sin(\theta) \\ \sin(\theta) & \cos(\theta) \end{bmatrix} \tag{A.15}$$

The transformation Eq. (A.13) can be written in vector form

$$\underline{v}^{(dq)}(t) = \mathrm{e}^{-\mathrm{j}\theta(t)} \underline{v}^{(\alpha\beta)}(t) \tag{A.16}$$

and the inverse Eq. (A.14) becomes

$$\underline{v}^{(\alpha\beta)}(t) = \mathrm{e}^{\mathrm{j}\theta(t)} \underline{v}^{(dq)}(t) \tag{A.17}$$

Some useful projection matrix translations are

$$\begin{matrix} \mathbf{R}^T(\theta) = \mathbf{R}(-\theta) & \mathbf{R}^T(\theta)\mathbf{R}(\theta) = \begin{bmatrix} 1 & 0 \\ 0 & 1 \end{bmatrix} \\ \mathbf{R}(\theta)\mathbf{R}(\theta) = \mathbf{R}(2\theta) & \mathbf{R}(-\theta)\mathbf{R}(-\theta) = \mathbf{R}(-2\theta) \end{matrix} \tag{A.18}$$

A.4 Voltage and Current Vectors in αβ– and *dq*-systems

Suppose that a symmetrical sinusoidal three-phase voltage, with the angular frequency ω_g, is transformed into a vector $\underline{u}(t) = u_\alpha(t) + \mathrm{j}u_\beta(t)$ in the αβ-frame. Define the *q*-axis in the dq-frame as parallel to the voltage vector $\underline{u}(t)$. This definition orginates from a flux vector parallel to the d-axis in the dq-frame. The voltage vector is proportional to the time derivative of the flux vector. As a consequence of the chosen reference vector, the voltage vector $\underline{u}(t)$ will only contain a q-component in the dq-frame. The transformation equation for a current vector from the αβ-frame to the dq-frame becomes, in matrix form

$$\begin{bmatrix} i_d(t) \\ i_q(t) \end{bmatrix} = \mathbf{R}\left(-\left(\omega_g t - \frac{\pi}{2}\right)\right)\begin{bmatrix} i_\alpha(t) \\ i_\beta(t) \end{bmatrix} \quad \text{(A.19)}$$

and the inverse

$$\begin{bmatrix} i_\alpha(t) \\ i_\beta(t) \end{bmatrix} = \mathbf{R}\left(\omega_g t - \frac{\pi}{2}\right)\begin{bmatrix} i_d(t) \\ i_q(t) \end{bmatrix} \quad \text{(A.20)}$$

Of course the voltage vector transformations from the αβ-frame to the dq-frame will be the same as those for the current vectors.

A.5 Positive-, Negative- and Zero-phase Sequence Harmonics

Harmonics in a three-phase system transformed to the αβ-frame will rotate in different directions depending on the harmonic number. For instance, the fundamental current will rotate counter-clockwise; the 5th harmonic currents will rotate clockwise and the 7th harmonic current will rotate counter-clockwise. The three voltage vectors in the αβ-frame are shown in Fig. A.3. The rotation directions of the different sequence harmonics are marked.

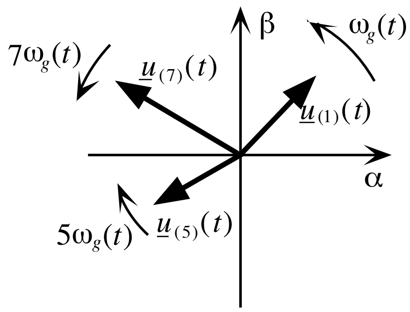

Figure A.3: The direction of different harmonics in the αβ-frame.

Harmonics of the orders $n = 3k, \quad k = 1,2,3,...$ are of a zero sequence. In the αβ-frame this harmonic vector will not rotate. In a three-phase grid without a neutral conductor, no zero-sequence harmonics will occur.

Harmonics of the order $n = 6k + 1, \quad k = 1,2,3,...$ are of a positive sequence. Thus, the harmonic vector in the αβ-frame will rotate counter-clockwise. For the lowest-order frequencies, the positive-sequence harmonics are the 7th, 13th and 19th.

Harmonics of the order $n = 6k - 1, \quad k = 1,2,3,...$ are of a negative sequence and the harmonic vector rotates clockwise in the αβ-frame. For the lowest-order frequencies, the negative-sequence harmonics are the 5th, 11th and 17th.

A.5.1 Harmonics in the *dq*-frame

When transforming vectors from the αβ-frame to the *dq*-frame, a counter-clockwise rotation of the αβ-frame with fundamental angular frequency will occur. The current vector $\underline{i}^{(\alpha\beta)}$ is transformed using

$$\underline{i}^{(dq)} = \mathrm{e}^{-\mathrm{j}(\omega_g t - \pi/2)} \underline{i}^{(\alpha\beta)} \tag{A.21}$$

The fundamental current vector in the αβ-frame will be transformed to a stationary vector in the *dq*-frame. Positive-sequence harmonics will rotate slower in the *dq*-frame. For negative-sequence harmonics, the vectors in the αβ-frame will rotate faster in the *dq*-frame. The harmonics transformation from the αβ-frame to the *dq*-frame are shown in Table A.2.

TABLE A.2

HARMONICS TRANSFORMATION FROM αβ-FRAME TO *DQ*-FRAME.

Harmonic type	Harmonic number n	αβ-frame	*dq*-frame
fundamental	n=1	$\underline{i}_{(1)}^{(\alpha\beta)}(t) = \hat{i}_{(1)} \mathrm{e}^{\mathrm{j}(\omega_g t - \pi/2)}$	$\underline{i}_{(1)}^{(\alpha\beta)}(t) = \hat{i}_{(1)}$
positive sequence	$n = 6k + 1$, $k = 1,2,3,\ldots$	$\underline{i}_{(n)}^{(\alpha\beta)}(t) = \hat{i}_{(1)} \mathrm{e}^{\mathrm{j}n(\omega_g t - \pi/2)}$	$\underline{i}_{(n)}^{(dq)}(t) = \hat{i}_{(n)} \mathrm{e}^{\mathrm{j}(n-1)(\omega_g t - \pi/2)}$
negative sequence	$n = 6k - 1$, $k = 1,2,3,\ldots$	$\underline{i}_{(n)}^{(\alpha\beta)}(t) = \hat{i}_{(n)} \mathrm{e}^{-\mathrm{j}n(\omega_g t - \pi/2)}$	$\underline{i}_{(n)}^{(dq)}(t) = \hat{i}_{(n)} \mathrm{e}^{-\mathrm{j}(n+1)(\omega_g t - \pi/2)}$

A.6 References

[1] M. P. Kazmierkowski, H. Tunia, *Automatic Control of Converter-Fed Drives*, PWN–Polish Scientific Publishers, Warszawa Polen, 1994, p. 559.

PART II

INCLUDED PAPERS

SECTION 1
Voltage Source Converters in Variable Speed Wind Turbines and Hybrid Wind Parks

SECTION 2
Voltage Angle Control of a Voltage Source Converter

SECTION 3
Vector Controlled Voltage Source Converter

SECTION 4
Connecting Fast Switching Voltage Source Converters to the Grid

PAPER 1A

O. Carlson, A. Grauers, J. Svensson, Å. Larsson, "A Comparison of Electrical Systems for Variable Speed Operation of Wind Turbines," *European Wind Energy Association Conference and Exhibition (EWEC'94)*, Thessaloniki, Greece, 10-14 October 1994, pp. 500-505.

PAPER 1B

J. Svensson, "Possibilities by using a Self-commutated Voltage Source Inverter Connected to a Weak Grid in Wind Parks," *1996 European Union Wind Energy Conference and Exhibition*, Göteborg, Sweden, 20-24 May 1996, pp. 492-495.

PAPER 1C

J. Svensson, "The Rating of the Voltage Source Inverter in a Hybrid Wind Park with High Power Quality," *European Wind Energy Conference (EWEC'97)*, Dublin, Ireland, 6-9 October 1997, (in press).

PAPER 2A

J. Svensson, "Voltage Angle Control of a Voltage Source Inverter — Application to a Grid-Connected Wind Turbine," *6th European Conference on Power Electronics and Applications (EPE'95)*, Sevilla, Spain, 19-21 September 1995. Proceedings, Vol. 3, pp. 539-544.

PAPER 2B

J. Svensson, "Simulation of Power Angle Controlled Voltage Source Converter using a Linear Quadratic Method in a Wind Energy Application," *5th Workshop on Computers in Power Electronics, IEEE,* 11-14 August 1996, pp. 157-162.

PAPER 3A

J. Svensson, "Inclusion of Dead-Time and Parameter Variations in VSC Modelling for Predicting Responses of Grid Voltage Harmonics," *7th European Conference on Power Electronics and Applications (EPE'97)*, Trondheim, Norway, 8-10 September 1997, Proceedings, Vol. 3, pp. 216-221.

PAPER 3B

J. Svensson, "Synchronisation Methods for Grid Connected Voltage Source Converter," Submitted to IEE Proceedings Electric Power Applications.

PAPER 3C

J. Svensson, M. Lindgren, "Influence of Non-linearities on the Frequency Response of a Grid-Connected Vector-Controlled VSC," submitted to IEEE Transactions on Industrial Electronics.

PAPER 4

M. Lindgren, J. Svensson, "Connecting Fast Switching Voltage-source Converters to the Grid — Harmonic Distortion and its Reduction," *IEEE/Stockholm Power Tech Conference*, Stockholm, Sweden, June 18-22 1995. Proceedings, Vol. "Power Electronics", pp. 191-196.